SUPPORTING INFORMATION FOR:

# Versatile organoaluminium catalysts based on heteroscorpionate ligands for the preparation of polyesters

*J. Martínez,[a] M. Martínez de Sarasa Buchaca,[a] F. de la Cruz-Martínez,[a] C. Alonso-Moreno,[b] L. F. Sánchez-Barba,[c] J. Fernandez-Baeza,[a] A. M. Rodríguez,[a] A. Rodríguez-Diéguez,[d] J. A. Castro-Osma,*[b] A. Otero*[a] and A. Lara-Sánchez[a]**

*[a]Universidad de Castilla-La Mancha. Dpto. de Química Inorgánica, Orgánica y Bioquímica, Facultad de Ciencias y Tecnologías Químicas, 13071-Ciudad Real, Spain. E-mail: Agustin.Lara@uclm.es, Antonio.Otero@uclm.es*

*[b]Universidad de Castilla-La Mancha. Dpto. de Química Inorgánica, Orgánica y Bioquímica, Facultad de Farmacia, 02071-Albacete, Spain. E-mail: JoseAntonio.Castro@uclm.es*

*[c]Universidad Rey Juan Carlos, Departamento de Biología y Geología, Física y Química Inorgánica, Móstoles, 28933 Madrid, Spain.*

*[d]Dpto. de Química Inorgánica, Facultad de Ciencias, Universidad de Granada, Avda. de Fuentenueva s/n, 18071-Granada Spain.*

# Table of Contents

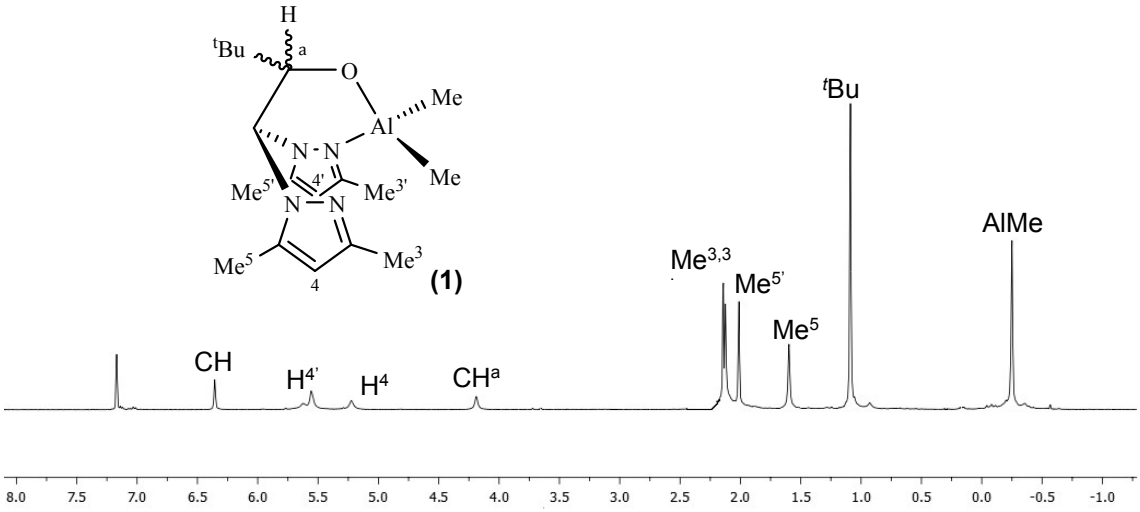


**Figure S1.** $^1$H-NMR Spectrum for complex **1** in $C_6D_6$**.**

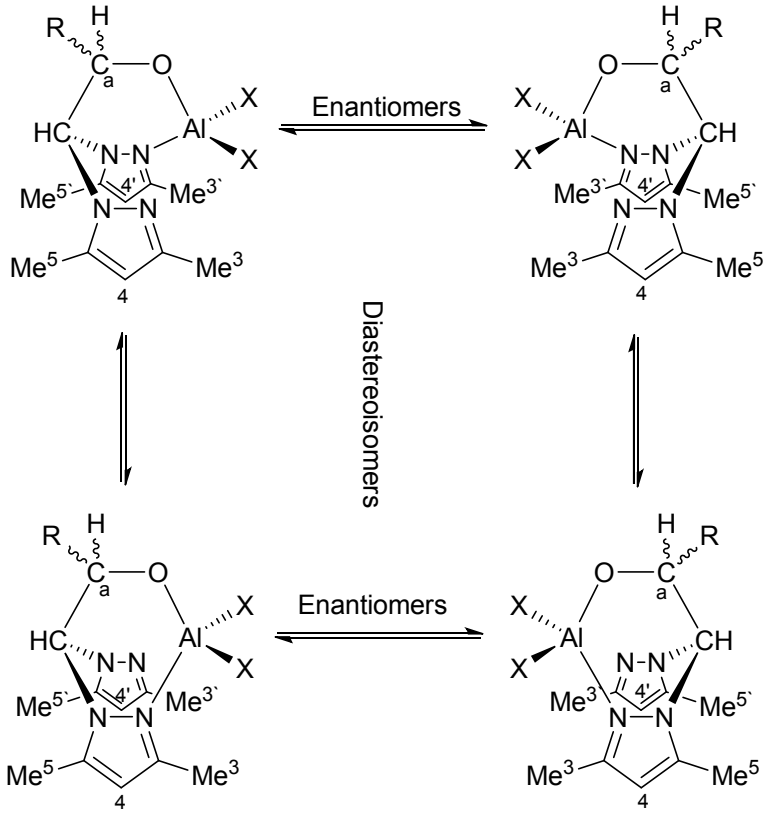


**Figure S2.** Fluxional behaviour as a result of a slow exchange process between the coordinated and non-coordinated pyrazole rings for complexes **1**-**4**.

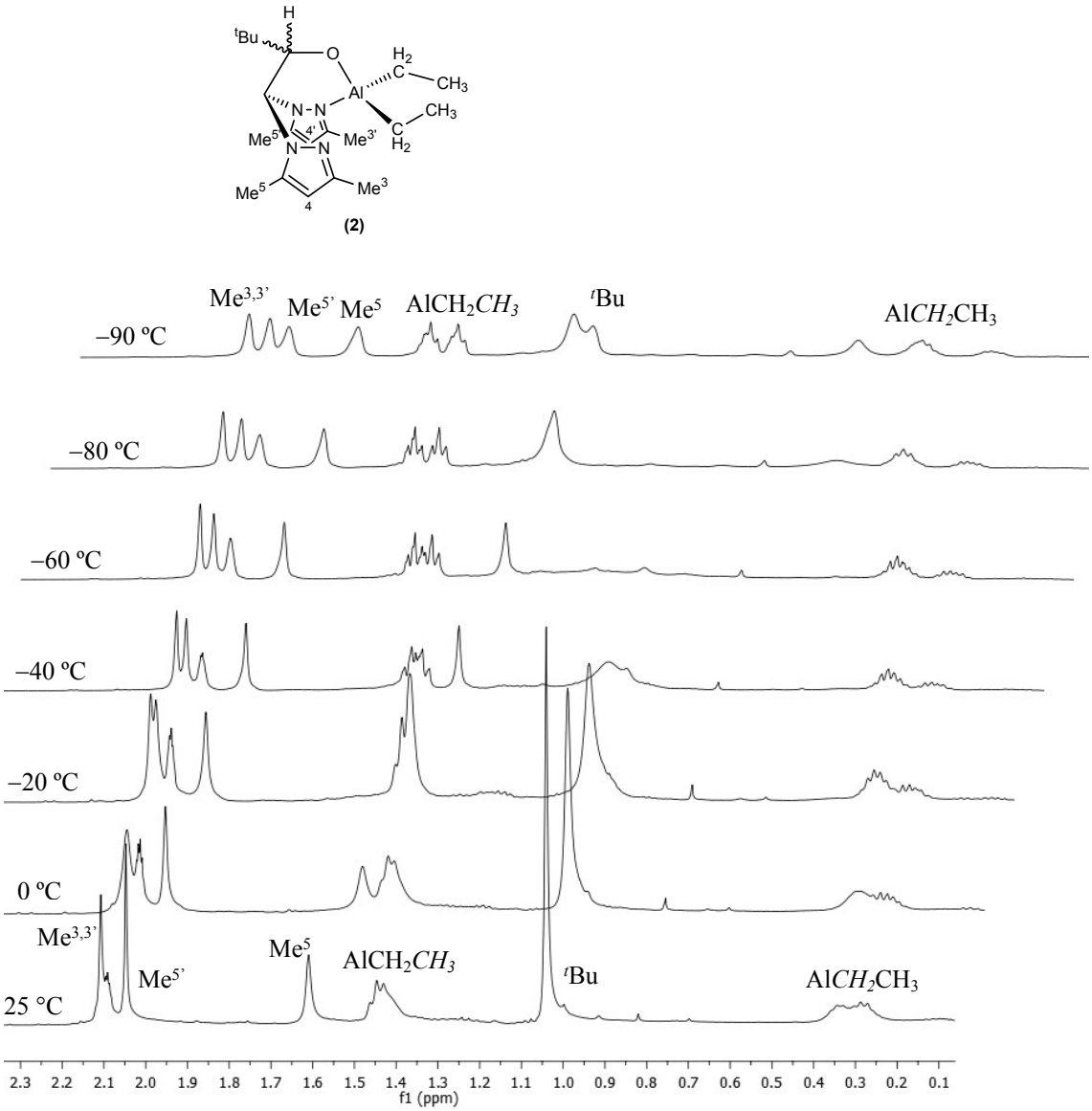


**Figure S3.** VT-NMR study in the region from 2.4 to 0.0 ppm for compound **2** in toluene-$d_8$. The VT NMR analysis showed that the resonances of the pyrazole rings and the alkyl groups broaden and become resolved indicating the presence of two diastereoisomers at –90 ºC. Therefore, there is an exchange process between the coordinated and the non-coordinated pyrazole rings, involving an interconversion from one diastereoisomer to the other. It is worth mentioning that the methine carbon bridging the two pyrazole rings is a stereocentre due to the coordination mode of heteroscorpionate ligand.

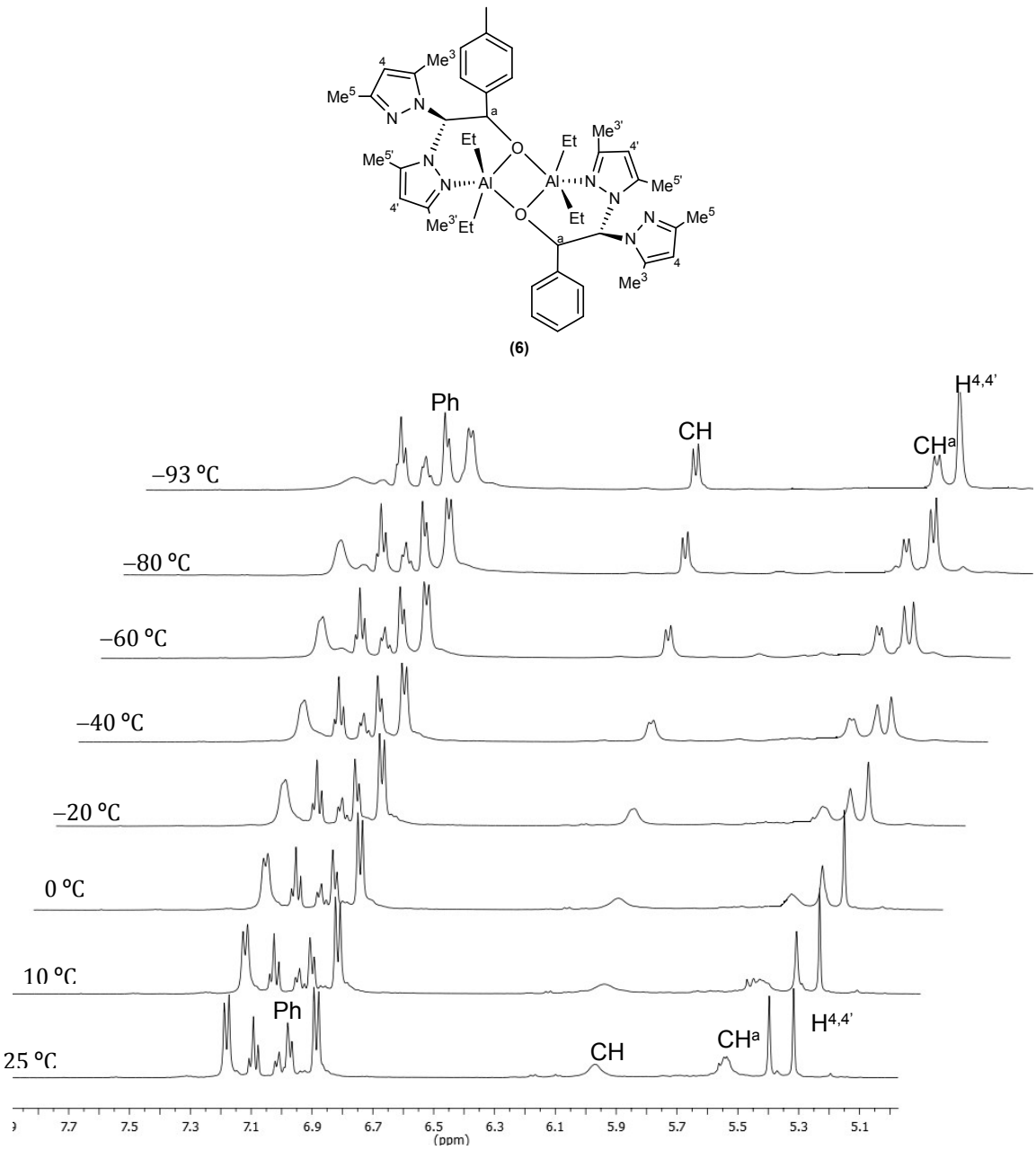


**Figure S4.** VT-NMR study in the region from 8.0 to 5.1 ppm for compound **6** in toluene-$d_8$. The VT NMR analysis showed that the resonances of the pyrazole rings become resolved indicating the presence of onediastereoisomers at –90 ºC. Therefore, there is not an exchange process between the coordinated and the non-coordinated pyrazole rings.

**Table S1.** Crystal data and structure refinement for compounds **1** and **5**

| | **1** | **5** |
|---|---|---|
| Empirical formula | $C_{18}H_{31}AlN_4O$ | $C_{49}H_{66}Al_2N_8O_2$ |
| Formula weight | 346.45 | 853.05 |
| Temperature (K) | 230(2) | 100(2) |
| Wavelength (Å) | 0.71073 | 0.71073 |
| Crystal system | Triclinic | Triclinic |
| Space group | P $\bar{1}$ | P $\bar{1}$ |
| a(Å) | 8.913(5) | 10.3817(6) |
| b(Å) | 9.995(6) | 10.7672(7) |
| c(Å) | 12.184(8) | 10.8726(7) |
| α(°) | 93.893(13) | 102.164(2) |
| β(°) | 97.531(13) | 95.020(2) |
| γ(°) | 101.566(16) | 91.554(2) |
| Volume(Å$^3$) | 1049.2(11) | 1182.22(13) |
| Z | 2 | 1 |
| Density (calculated) (g/cm$^3$) | 1.097 | 1.198 |
| Absorption coefficient (mm$^{-1}$) | 0.108 | 0.109 |
| F(000) | 376 | 458 |
| Crystal size (mm$^3$) | 0.23 x 0.17 x 0.12 | 0.20 x 0.20 x 0.14 |
| Index ranges | $-11 \leq h \leq 9$<br>$-7 \leq k \leq 12$<br>$-15 \leq l \leq 15$ | $-12 \leq h \leq 12$<br>$-13 \leq k \leq 13$<br>$-13 \leq l \leq 13$ |
| Reflections collected | 6894 | 15102 |
| Independent reflections | 4512 [R(int) = 0.0227] | 4644 [R(int) = 0.0493] |
| Data / restraints / parameters | 4512 / 0 / 226 | 4644 / 0 / 315 |
| Goodness-of-fit on F$^2$ | 1.063 | 1.038 |
| Final R indices [$I>2\sigma(I)$] | R1 = 0.0559, wR2 = 0.1363 | R1 = 0.0418, wR2 = 0.0936 |
| Largest diff. peak / hole, e.Å$^{-3}$ | 0.208 / -0.175 | 0.349 / -0.214 |

[a] $R = \Sigma||F_o|-|F_c|/\Sigma|F_o|$. [b] $wR = \{\Sigma w(F_o^2-F_c^2)^2/\Sigma w(F_o^2)^2\}^{1/2}$. [c] GOF = $\{\Sigma\ [w((F_o^2-F_c^2)^2)/(n-p)\}^{1/2}$, where $n$ = number of reflections and $p$ = total number of parameters refined.

**Table S2.** Bond distances (Å) and angles (º) for compound **1** and **5**

| **Bond Distances** | | | |
|---|---|---|---|
| **1** | | **5** | |
| Al(1)-O(1) | 1.7575(19) | Al(1)-O(1) | 1.8388(12) |
| Al(1)-C(17) | 1.964(3) | Al(1)-C(1) | 1.9883(18) |
| Al(1)-C(18) | 1.970(3) | Al(1)-C(2) | 1.9841(17) |
| Al(1)-N(1) | 2.004(2) | Al(1)-N(1) | 2.1436(15) |
| | | Al(1)-O(1A)[a] | 1.9936(12) |
| **Bond Angles** | | | |
| O(1)-Al(1)-C(17) | 112.55(11) | O(1)-Al(1)-C(2) | 129.92(7) |
| O(1)-Al(1)-C(18) | 114.13(10) | O(1)-Al(1)-C(1) | 114.48(7) |
| C(17)-Al(1)-C(18) | 118.62(12) | C(2)-Al(1)-C(1) | 115.43(8) |
| O(1)-Al(1)-N(1) | 92.25(7) | O(1)-Al(1)-O(1A)[a] | 74.44(5) |
| C(17)-Al(1)-N(1) | 108.80(11) | C(2)-Al(1)-O(1A)[a] | 95.34(6) |
| C(18)-Al(1)-N(1) | 106.86(11) | C(1)-Al(1)-O(1A)[a] | 97.49(6) |
| | | O(1)-Al(1)-N(1) | 86.37(5) |
| | | C(2)-Al(1)-N(1) | 92.39(7) |
| | | C(1)-Al(1)-N(1) | 95.89(7) |
| | | O(1A)[a]-Al(1)-N(1) | 159.89(6) |

[a] Symmetry transformations used to generate equivalent atoms: -x+1,-y+1,-z+1

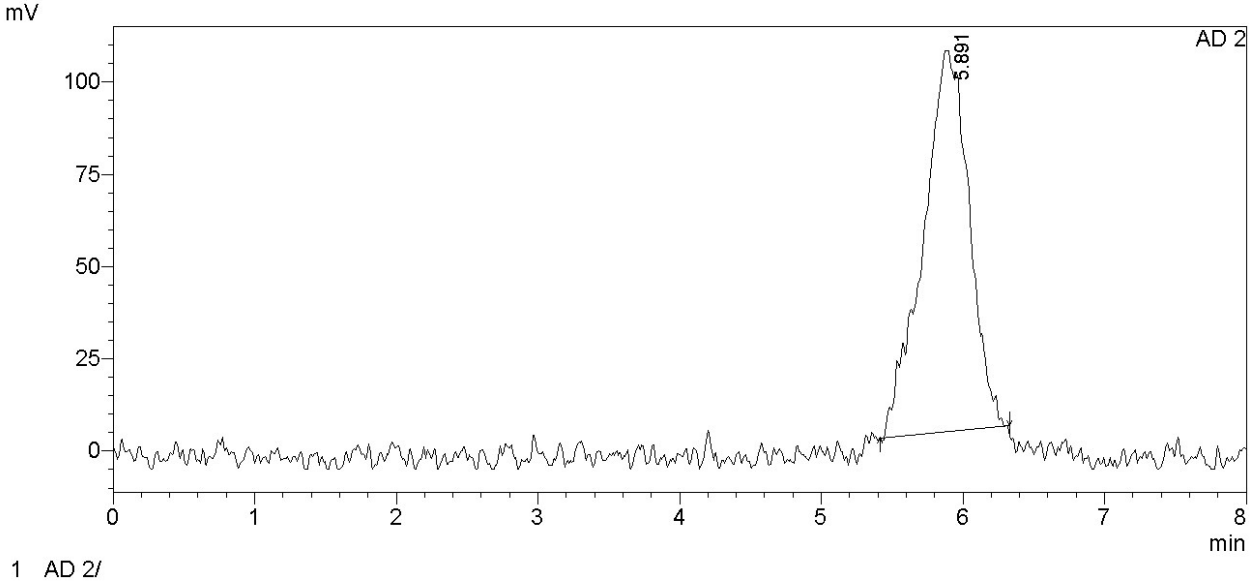


GPC Summary

Chromatogram AD 2

| # | Title | Mn | Mw | Mz | Mz1 | Mv |
|---|---|---|---|---|---|---|
| 1 | 40.lcd | 18797 | 19983 | 21746 | 24287 | 0 |
| | Average | 18797 | 19983 | 21746 | 24287 | 0 |
| | %RSD | 0.000 | 0.000 | 0.000 | 0.000 | 0.000 |
| | Maximum | 18797 | 19983 | 21746 | 24287 | 0 |
| | Minimum | 18797 | 19983 | 21746 | 24287 | 0 |
| | SD | 0 | 0 | 0 | 0 | 0 |

**Figure S5.** GPC profile of PCL with $M_n$ = 18797 Da and $M_w/M_n$ = 1.06 (entry 6 in Table 1)

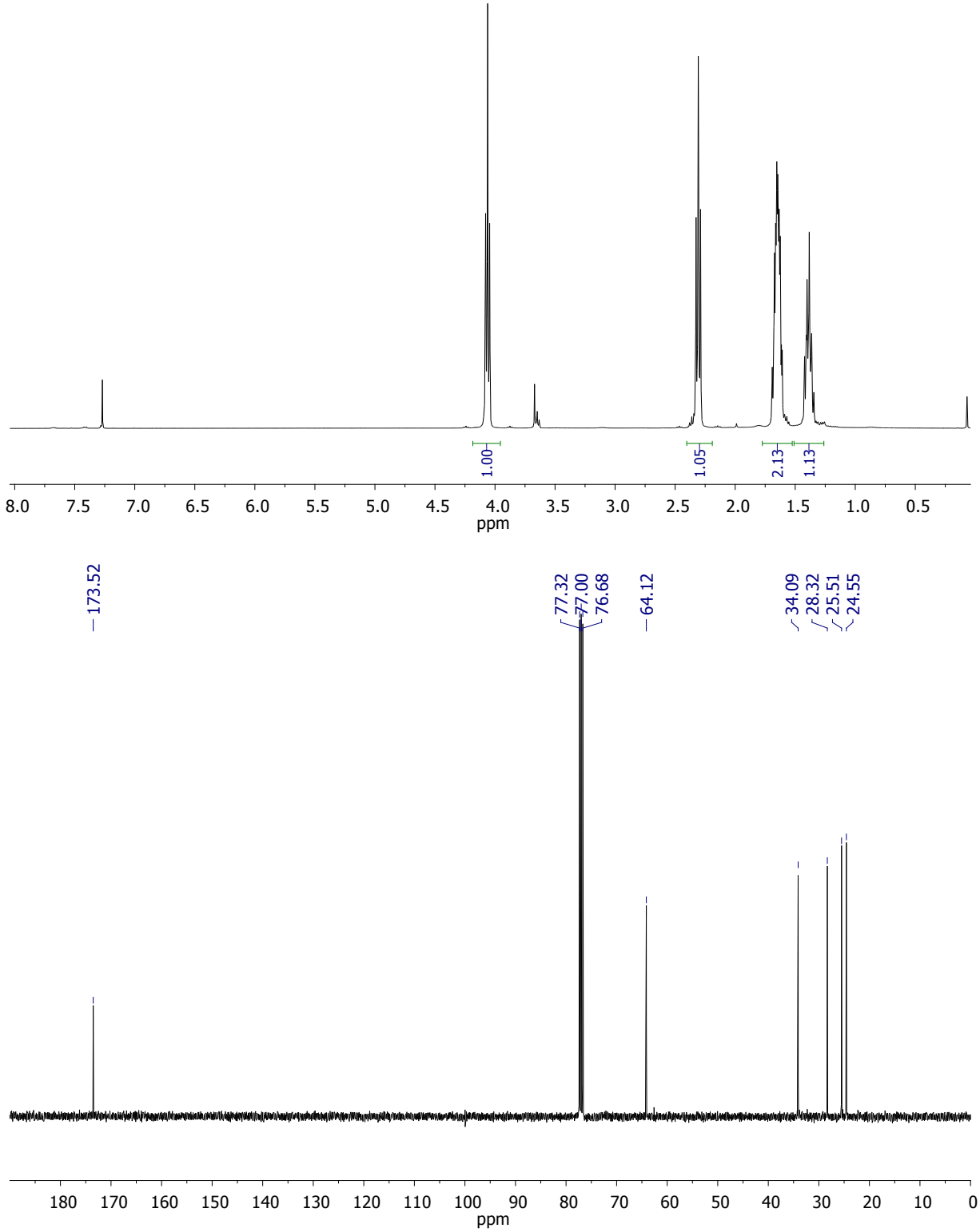


**Figure S6**. NMR spectra of PCL with $M_n$ = 18797 Da and $M_w/M_n$ = 1.06 prepared with complex **6**

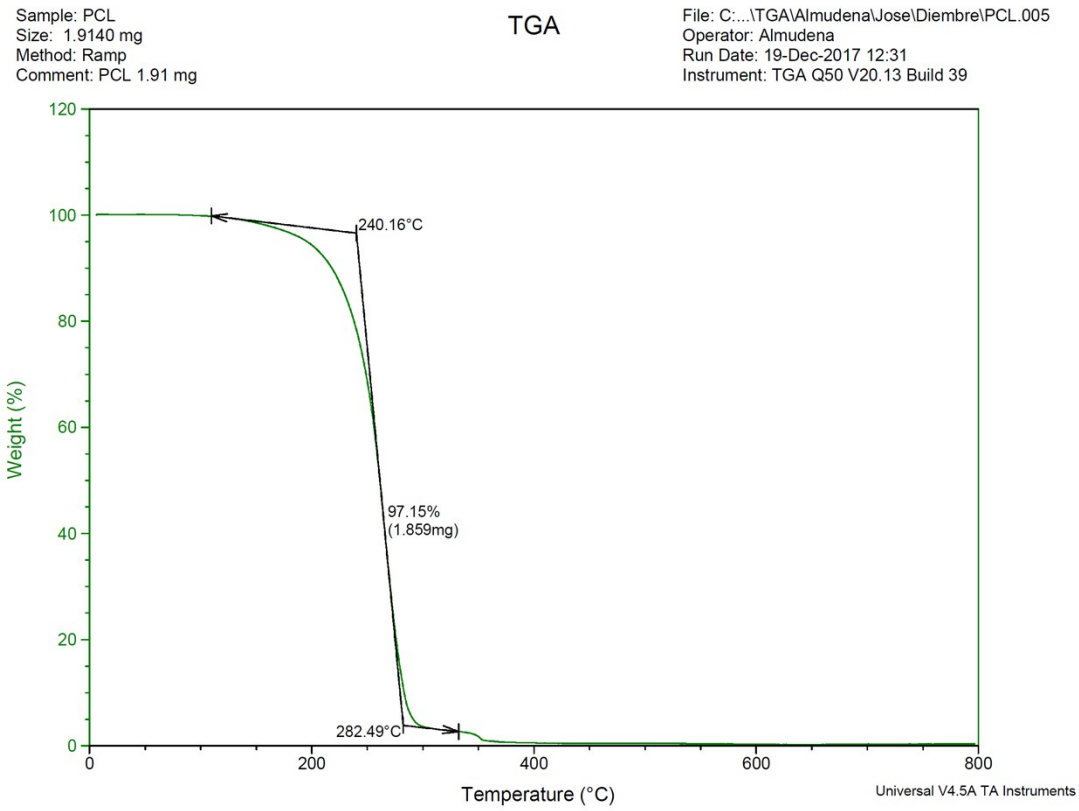


**Figure S7**. TGA analysis of PCL with $M_n$ = 18797 Da and $M_w/M_n$ = 1.06 prepared with complex **6**

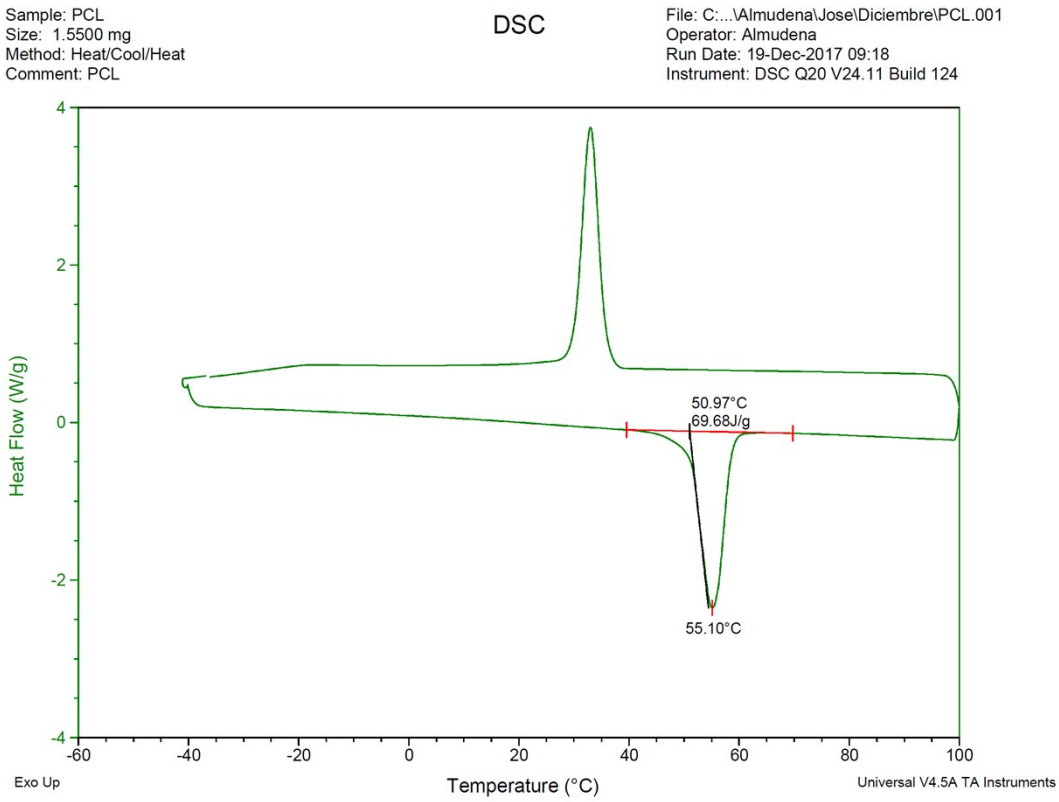

**Figure S8**. DSC analysis of PCL with $M_n$ = 18797 Da and $M_w/M_n$ = 1.06 prepared with complex **6**

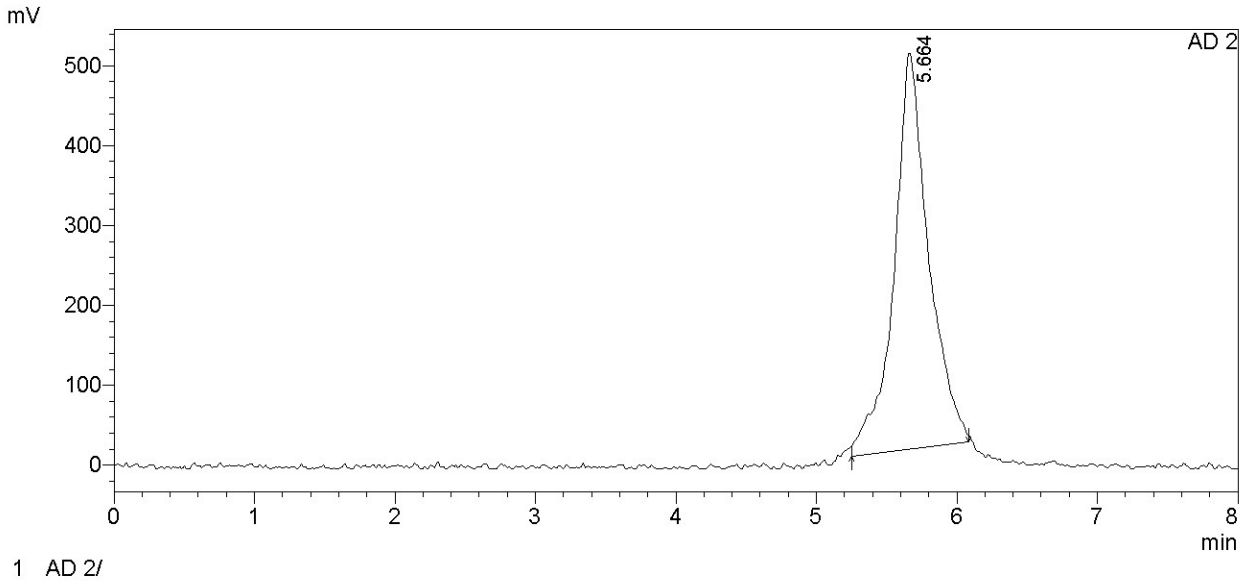


GPC Summary

Chromatogram AD 2

| # | Title | Mn | Mw | Mz | Mz1 | Mv |
|---|---|---|---|---|---|---|
| 1 | 41.lcd | 25869 | 29550 | 36399 | 48564 | 0 |
| | Average | 25869 | 29550 | 36399 | 48564 | 0 |
| | %RSD | 0.000 | 0.000 | 0.000 | 0.000 | 0.000 |
| | Maximum | 25869 | 29550 | 36399 | 48564 | 0 |
| | Minimum | 25869 | 29550 | 36399 | 48564 | 0 |
| | SD | 0 | 0 | 0 | 0 | 0 |

**Figure S9**. GPC profile of PLA with $M_n$ = 25869 Da and $M_w/M_n$ = 1.14 (entry 2 in Table 2)

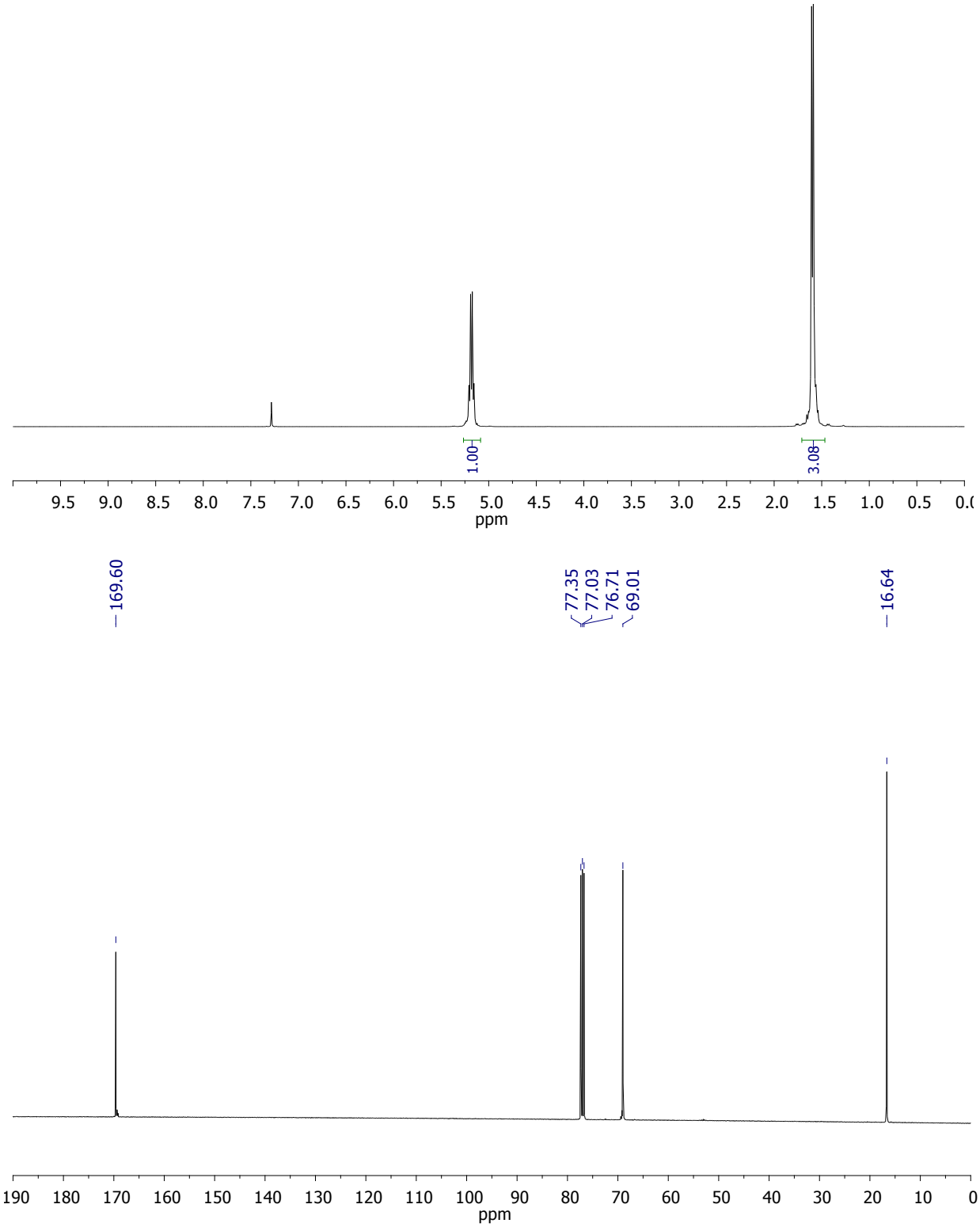


**Figure S10**. NMR spectra of PLA with $M_n$ = 25869 Da and $M_w/M_n$ = 1.14 prepared with complex **6**

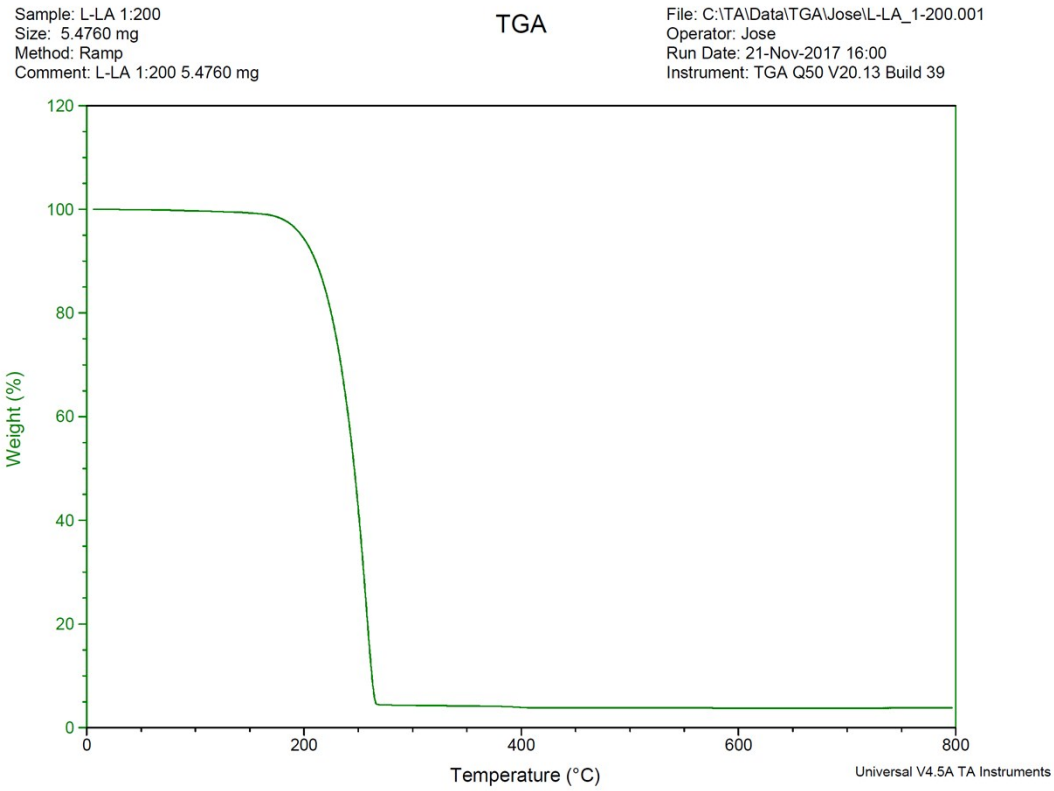


**Figure S11**. TGA analysis of PLA with $M_n$ = 25869 Da and $M_w/M_n$ = 1.14 prepared with complex **6**

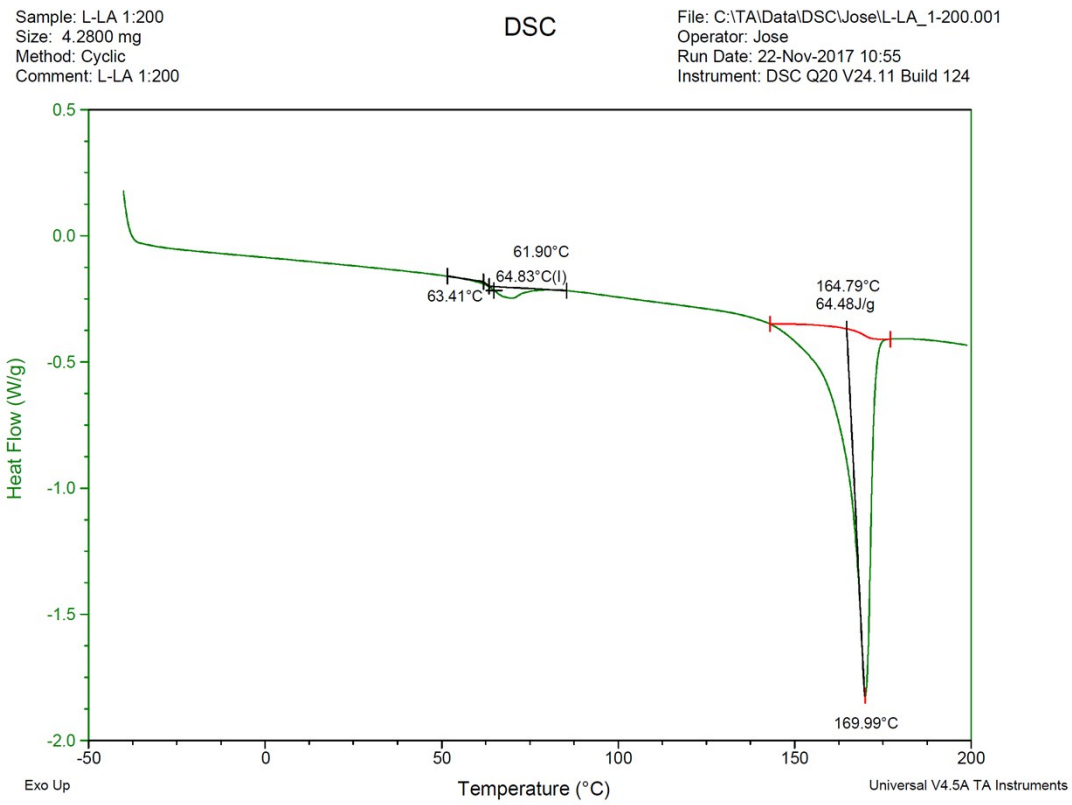

**Figure S12**. DSC analysis of PLA with $M_n$ = 25869 Da and $M_w/M_n$ = 1.14 prepared with complex **6**

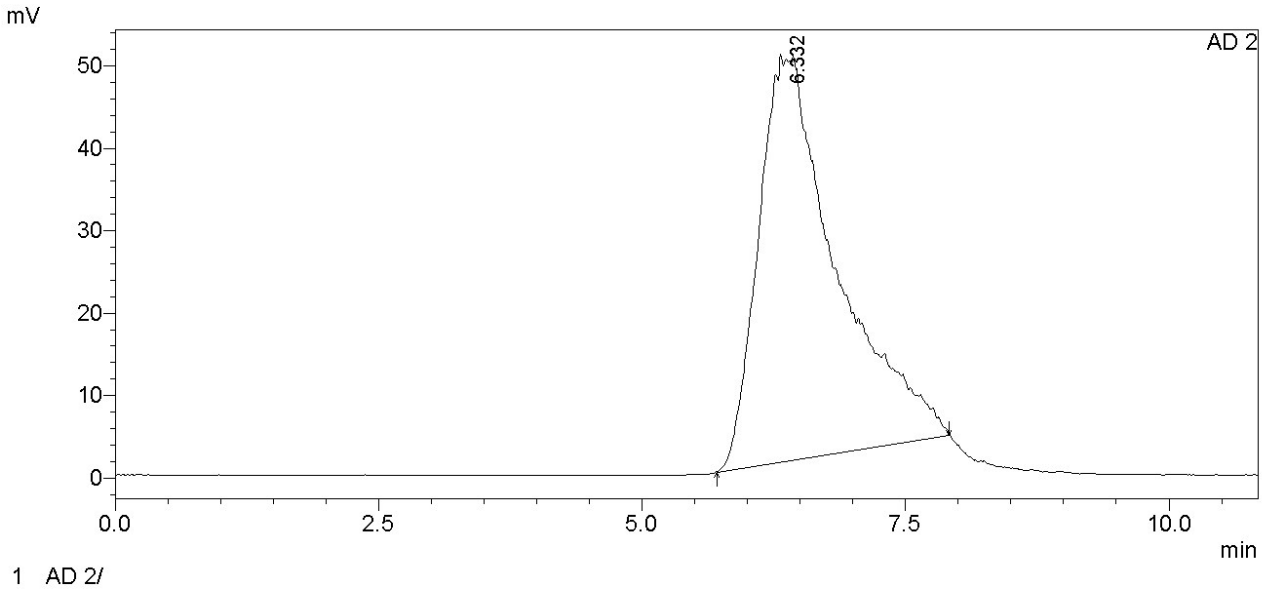


GPC Summary

Chromatogram AD 2

| # | Title | Mn | Mw | Mz | Mz1 | Mv |
|---|---|---|---|---|---|---|
| 1 | 75.lcd | 14744 | 15323 | 16172 | 17489 | 0 |
| | Average | 14744 | 15323 | 16172 | 17489 | 0 |
| | %RSD | 0.000 | 0.000 | 0.000 | 0.000 | 0.000 |
| | Maximum | 14744 | 15323 | 16172 | 17489 | 0 |
| | Minimum | 14744 | 15323 | 16172 | 17489 | 0 |
| | SD | 0 | 0 | 0 | 0 | 0 |

**Figure S13**. GPC profile of copolymer of cyclohexene oxide and phthalic anhydride with $M_n$ = 14744 Da and $M_w/M_n$ = 1.04 (entry 4 in Table 4)

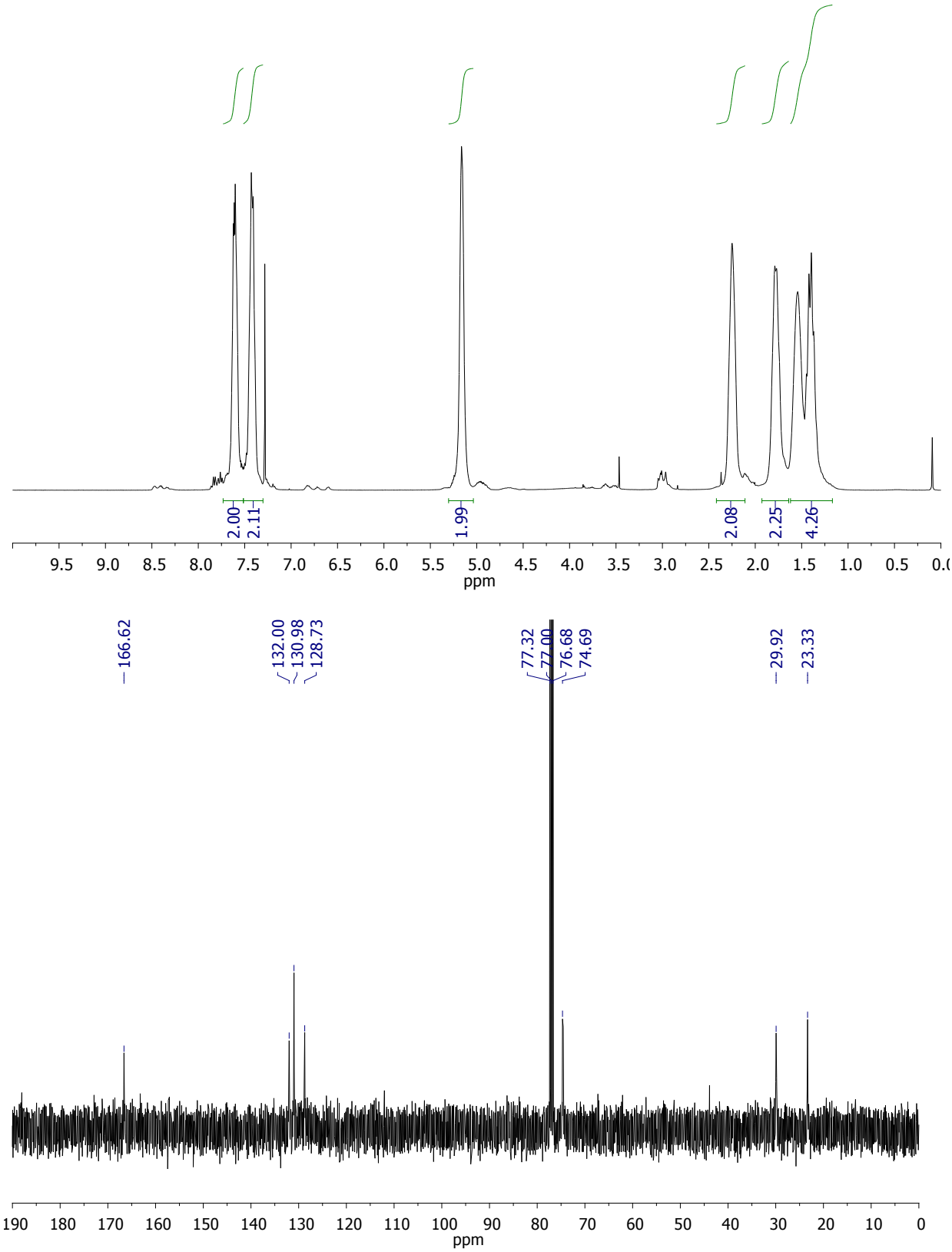


**Figure S14**. NMR spectra for copolymer of cyclohexene oxide and phthalic anhydride with $M_n$ = 14744 Da and $M_w/M_n$ = 1.04 prepared with complex **6**

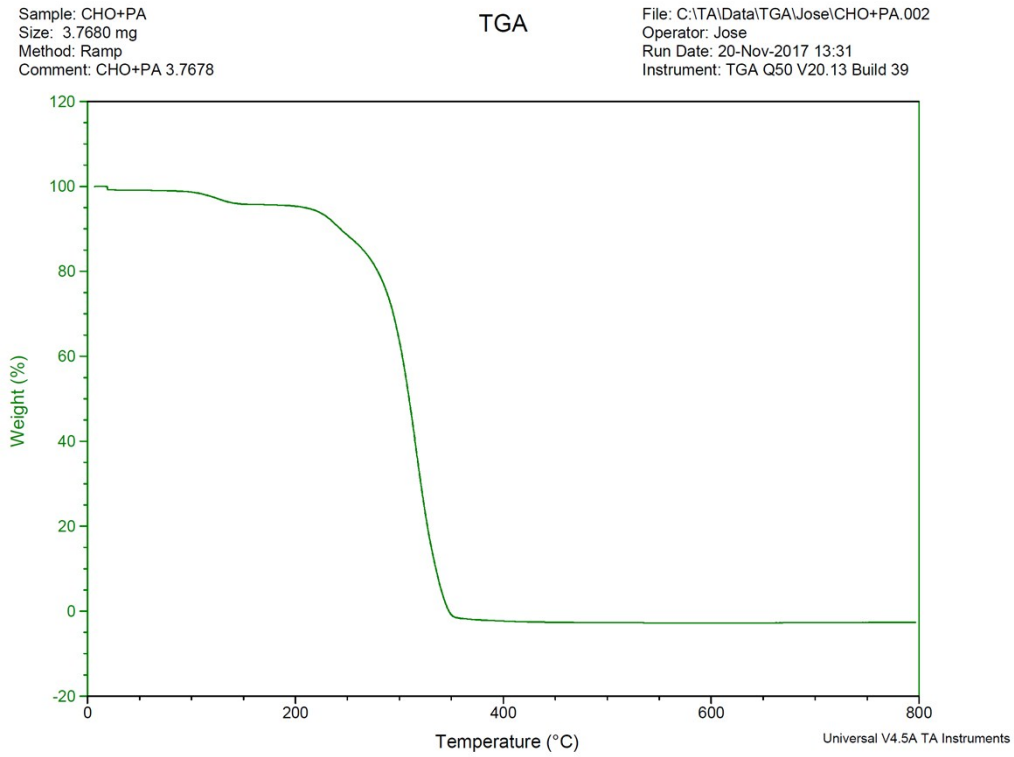


**Figure S15**. TGA analysis for copolymer of cyclohexene oxide and phthalic anhydride with $M_n$ = 14744 Da and $M_w/M_n$ = 1.04 prepared with complex **6**

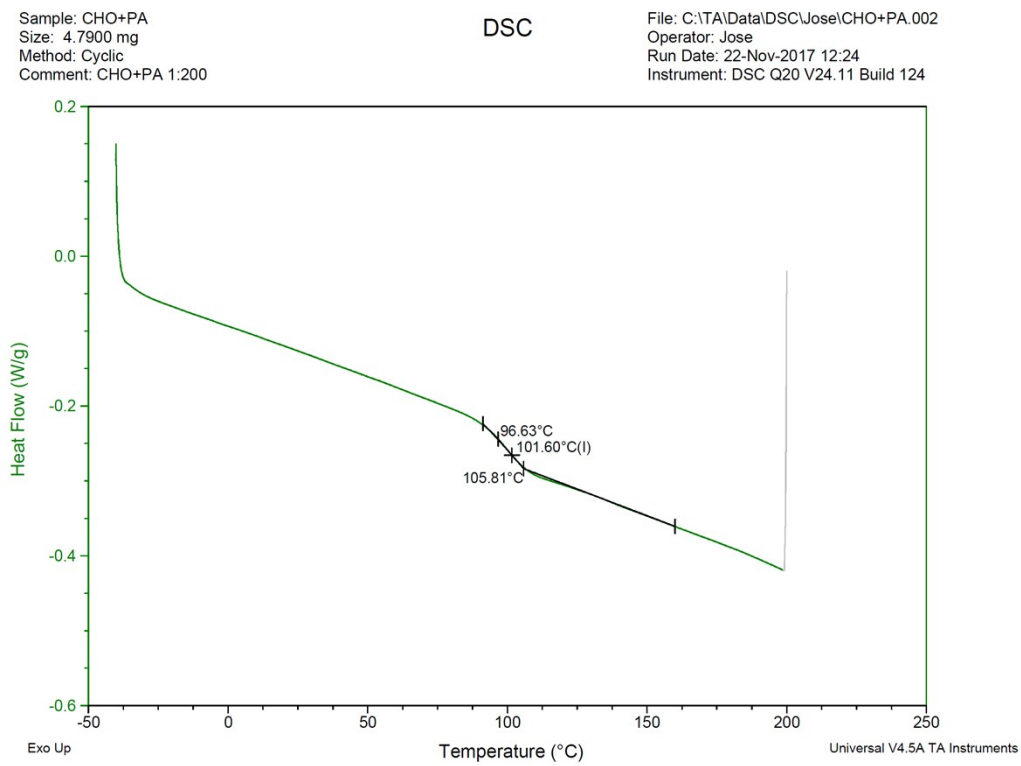

**Figure S16**. DSC analysis for copolymer of cyclohexene oxide and phthalic anhydride with $M_n$ = 14744 Da and $M_w/M_n$ = 1.04 prepared with complex **6**